Supporting Information

In-situ reduction of Cu nanoparticles on Mg-Al-LDH for simultaneous efficient catalytic transfer hydrogenation of furfural to furfuryl alcohol

Ganen Pan[a,‡], Shifang Cheng[a,‡], Yingxue Zhang[a], Yakai Chen[a], Xingliang Xu [a,b,*], Jing Xu [a,b,*]

[a] College of Chemistry and Material Science, Shandong Agricultural University, Taian 271018, P. R. China

[b] Key Laboratory of Agricultural Film Application of Ministry of Agriculture and Rural Affairs, Taian 271018, P. R. China

[‡] These authors contribute equally to this work.

* Corresponding author: Xingliang Xu: xxlsdau@163.com

Jing Xu: jiaxu@sdau.edu.cn

General Information

Materials

Sodium hydroxide (NaOH) and sodium carbonate (Na_2CO_3) was purchased from Tianjin chemical reagent factory. Copper nitrate hexahydrate ($Cu(NO_3)_2 \cdot 6H_2O$), aluminium nitrate nonahydrate ($Al(NO_3)_3 \cdot 9H_2O$) and magnesium nitrate hexahydrate ($Mg(NO_3)_2 \cdot 6H_2O$) were obtained from Sigma-Aldrich Inc. Methanol, ethanol 1-propanol, isopropanol and 2-butanol was purchased from Sinopharm Chemical Reagent Co. LTD. FAL ($C_5H_4O_2$) and FOL ($C_5H_6O_2$) was purchased from Shanghai Macklin Biochemical Co. Ltd. All chemical reagents were used as received and without further purification.

Synthesis of CuMgAl-LDH precursors

The $Cu_xMg_{3-x}Al_1$-LDH precursors (x=0,1.0,1.5,2.0,3.0) were obtained by the coprecipitation method. In a typical preparation, a mixture of $Cu(NO_3)_2 \cdot 6H_2O$ (0.015mol), $Mg(NO_3)_2 \cdot 6H_2O$ (0.015 mol) and $Al(NO_3)_3 \cdot 9H_2O$ (0.010 mol) were dissolved in 120 mL deionized water (the mole ratio of $Cu^{2+}:Mg^{2+}:Al^{3+}$ was 1.5:1.5:1). The mixed salt solution prepared above was dropwise added into 50 mL Na_2CO_3 solution (0.166 mol/L) in a 500 mL three-neck round bottom flask with mechanical stirring under air atmosphere, and the pH was maintained at around 10 by adding NaOH solution (1 mol/L). After the titration, the resulting suspension was further heated at 60 °C for 3 h under continuous magnetic stirring. The resulting precipitate was filtered, and then transferred into the 2.00 mol/L Na_2CO_3 solution (50 mL) and further heated at 40 °C for 12 h with mechanical stirring. The final precipitate after centrifugation was washed with decarbonated water and the residue was dried in vacuum at 80 °C for 24 h. Different proportions of $Cu_xMg_{3-x}Al_1$-LDHs were also prepared by the same method as above.

Catalyst Characterization

The crystalline structure of the catalyst before and after the reaction was obtained using X-ray Powder Diffractometer (Rigaku D/max-2550) with Cu Kα radiation and k = 1.5418 Å at scanning rate of 5° per second in the range from 10° to 80°.

The surface topography and corresponding EDX-mappings of catalyst was detected using a Sigma-300 scanning electron microscope (SEM) with an EDAX energy dispersive detector. The sample was transferred to Mo grid and then was observed by high-resolution transmission electron microscopy (HRTEM), which was taken by a Tecnai-F20 microscope at 200 kV.

The Fourier transform infrared (FTIR) spectra were recorded on a Bruker VERTEX 70 infrared spectrometer after tableting sample with KBr. X-ray photoelectron spectroscopy (XPS) was recorded on a Thermo ESCALAB 250xi spectrometer. The source of the radiation was Al Kα (1486.6 eV), and the binding energy (BE) was corrected at a C1S peak of 284.8 eV. The Brunauer−Emmet−Teller (BET) surface area was carried out by using a Quantachrome Autosorb-1C-VP analyzer. Bronsted and Lewis acid densities were determined by pyridine adsorption infrared (Py-IR) using a TENSOR 27 apparatus. The elemental compositions of catalysts were determined by inductively coupled plasma (ICP) with Optima 3300 DV (PerkinElmer Instruments).

Catalytic Testing

The catalytic transfer hydrogenation of FAL to FOL was carried out in a 50 mL steel alloy autoclave without stirring. In a standard procedure, the autoclave was loaded with FAL (0.10 mL), 2-PrOH (20 mL) and catalyst (0.1 g), then sealed into the oven and heated to the target temperature (100-180 °C) and reaction time (2-8 h). After the reaction, the autoclave was cooled to room temperature and opened to process the obtained liquid mixture. FAL conversion and FAL selectivity were calculated by GC 2010 gas chromatograph equipped with a hydrogen flame ionization detector. FAL conversion and FAL selectivity were calculated by the following equations:

The calculation formula of furfural conversion:

$$Con. = \frac{M_i - M_f}{M_i} \times 100\%$$

The calculation formula of furfuryl alcohol selectivity:

$$Sel. = \frac{N_f}{M_i - M_f} \times 100\%$$

M_i ：initial mol of FOL; M_f ：mol of FOL after reaction; N_f ：mol of the formed FOL.
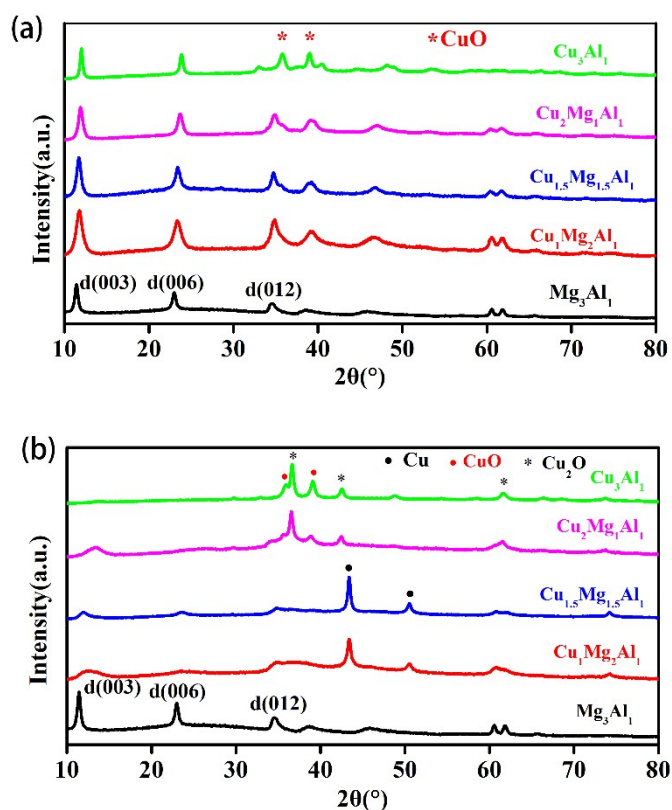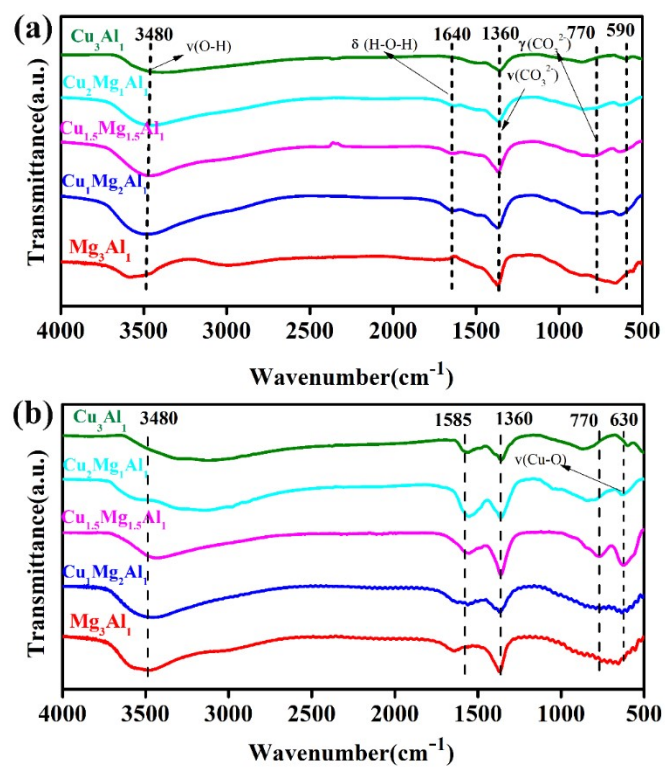

Fig. S1 XRD patterns of the fresh CuMgAl-LDH catalyst (a) and (b) in-situ reduced CuMgAl-LDH catalyst with different proportions. Reaction conditions: catalyst (0.1 g), FAL (0.1 mL), 2-PrOH (20 mL), 160 ℃, 6 h.

As shown in Fig. S1b, a large amount of Cu^{2+} are reduced to Cu^0, and the intensity of the diffraction peaks decreased and became broad, reflecting the decrease in the crystallinity of the LDH phase. In addition, Because Cu^{2+} and the interlayer counter ion CO_3^{2-} have the same valence number, LDHs can maintain the charge balance as well as the crystal structure by dissociating a Cu^{2+} and a CO_3^{2-} simultaneously during the in-situ reduction (*Applied Catalysis B: Environmental,2018, 224, 783-79*0).

Table. S1 Surface area, pore volume and average pore diameter of LDH precursor.

Entry	Catalyst

		BET surface (m²/g)	Pore diameter (nm)	Pore volume (cm³/g)
1	Mg_3Al_1-LDH	101.94	15.86	0.49
2	$Cu_1Mg_2Al_1$-LDH	112.27	30.24	1.04
3	$Cu_{1.5}Mg_{1.5}Al_1$-LDH	103.27	33.15	1.01
4	$Cu_2Mg_1Al_1$-LDH	86.27	31.69	0.79
5	Cu_3Al_1-LDH	64.23	30.11	0.54

Fig. S2 FT-IR spectra of the fresh CuMgAl-LDH catalyst (a) and (b) in-situ reduced CuMgAl-LDH catalyst with different proportions. Reaction conditions: catalyst (0.1 g), FAL (0.1 mL), 2-PrOH (20 mL), 160 ℃, 6 h.
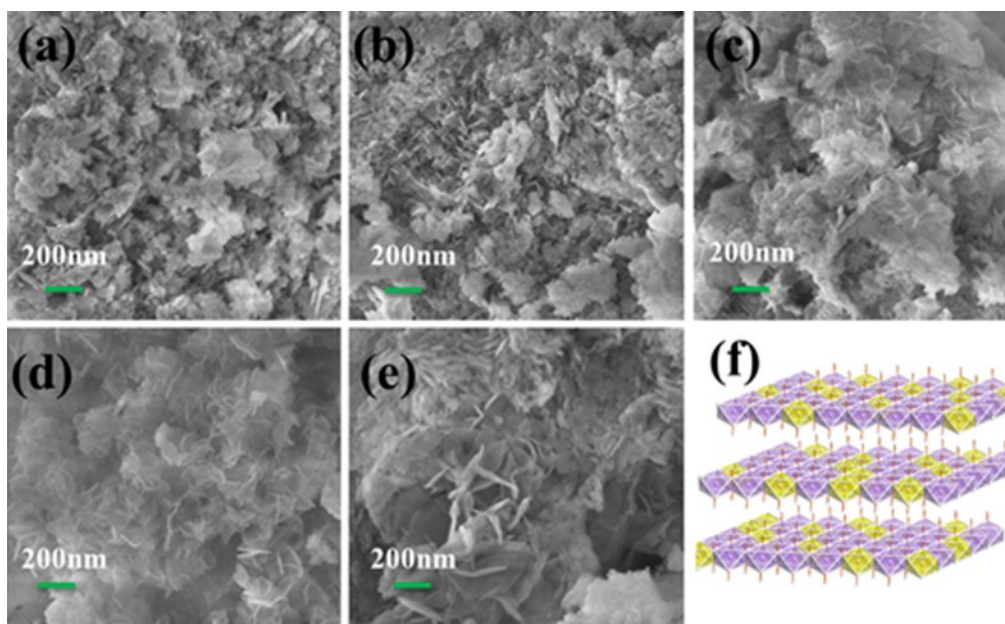
Fig. S3 SEM images of CuMgAl-LDH precursors with different Cu: Mg: Al ratios: (a) Cu_3Al_1-LDH, (b) $Cu_2Mg_1Al_1$-LDH, (c) $Cu_{1.5}Mg_{1.5}Al1$-LDH, (d) $Cu_1Mg_2Al_1$-LDH, (e) Mg_3Al_1-LDH, (f) Crystal structure of class hydrotalcite.
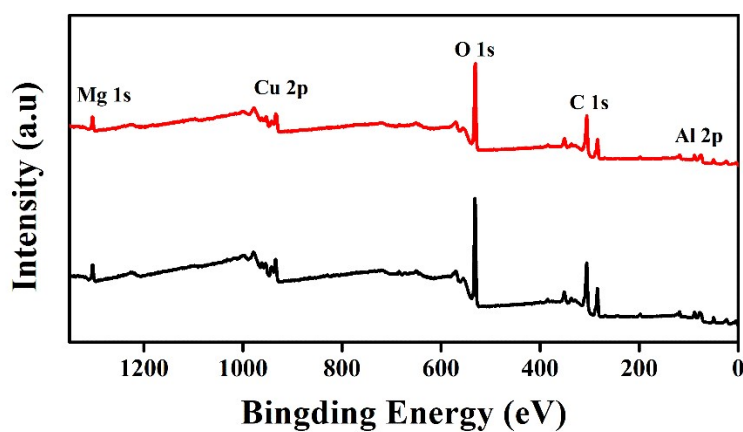
Fig. S4 XPS survey scan spectrum of the fresh $Cu_{1.5}Mg_{1.5}Al_1$-LDH (black line) and in situ reduced $Cu_{1.5}Mg_{1.5}Al_1$-LDH (red line).
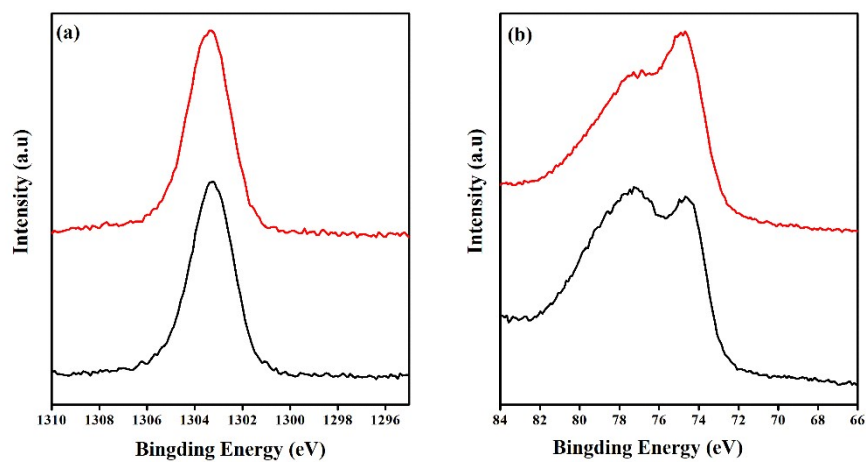
Fig. S5 XPS survey scan spectrum of the fresh $Cu_{1.5}Mg_{1.5}Al_1$-LDH (black line) and in situ reduced $Cu_{1.5}Mg_{1.5}Al_1$-LDH (red line).
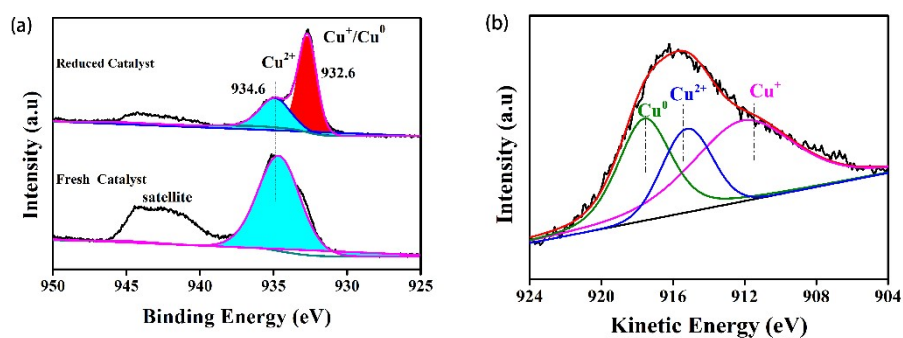
Fig. S6 (a) Cu 2p XPS spectra of the fresh $Cu_{1.5}Mg_{1.5}Al_1$-LDH catalyst and in-situ reduced $Cu_{1.5}Mg_{1.5}Al_1$-LDH catalyst. (b) Cu LMM Auger electron spectra for in-situ reduced $Cu_{1.5}Mg_{1.5}Al_1$-LDH catalyst.
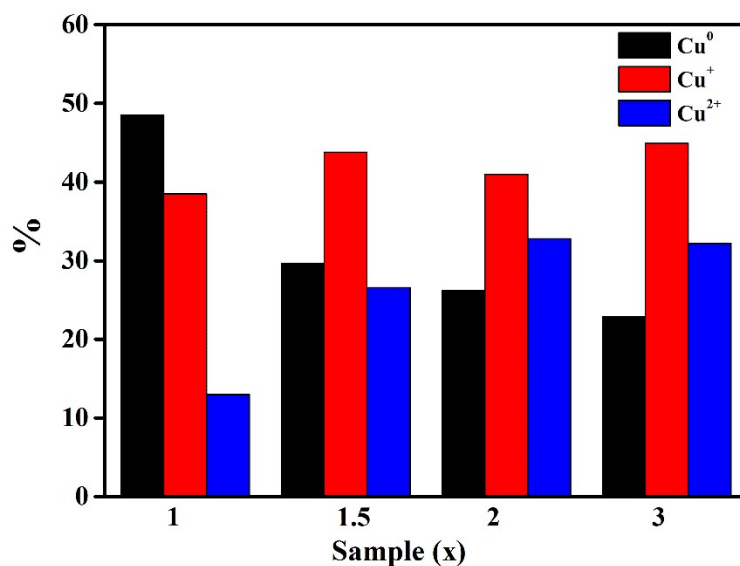
Fig. S7 The molar ratio of surface Cu^0: Cu^+: Cu^{2+} of the in-situ reduced CuMgAl-LDH catalyst with different proportions based on the Cu LMM Auger peak areas.
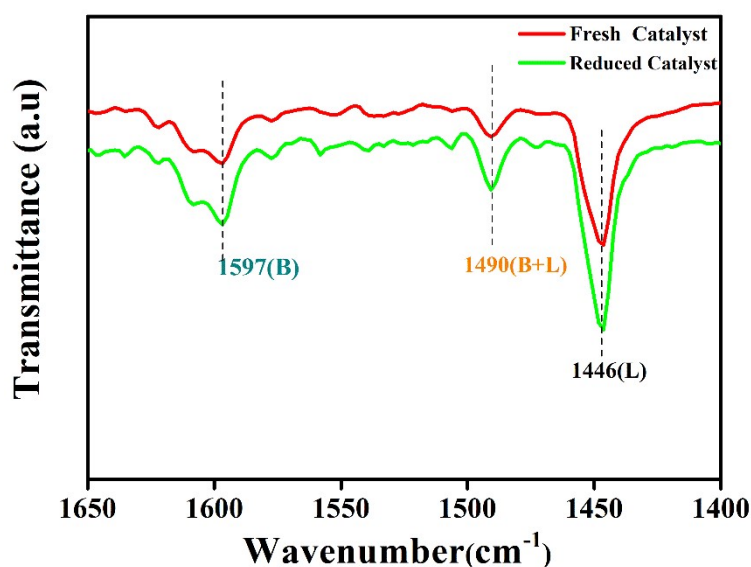

Fig. S8 Pyridine IR spectra of the fresh $Cu_{1.5}Mg_{1.5}Al_1$-LDH catalyst and in-situ reduced $Cu_{1.5}Mg_{1.5}Al_1$-LDH catalyst.

To gain more details of the specific acid sites over the fresh and in-situ reduction $Cu_{1.5}Mg_{1.5}Al_1$-LDH, the coexistence of Brønsted and Lewis acid sites were also determined by pyridine adsorption infrared (Py-IR). As seen in Fig. S8, the position of the spectra of pyridine adsorbed of $Cu_{1.5}Mg_{1.5}Al_1$-LDH before and after in-situ reduction basically did not change. Classically, the band at 1446 cm^{-1} can be assigned to Lewis acid sites. and the band at 1597 cm^{-1} was considered as arising from Brønsted acid sites. The band at 1490 cm^{-1} on samples were considered as due to the adsorption

of pyridine onto the coexistence of Brønsted and Lewis acid.

Table. S2 Catalytic transfer hydrogenation of FAL to FOL by various catalysts[a]

Entry	Catalyst	Conversion (%)[b]	Yield (%)[b]	Selectivity (%)[b]
1	Nothing	<1	--	--
2	Mg_3Al_1-LDH	24.6	20.2	82.4
3	$Cu_1Mg_2Al_1$-LDH	95	86	90
4	$Cu_{1.5}Mg_{1.5}Al_1$-LDH	99	97.5	98.2
5	$Cu_2Mg_1Al_1$-LDH	41.7	37.5	90.3
6	Cu_3Al_1-LDH	38.2	36.8	97.9
7[c]	$Cu_{1.5}Mg_{1.5}Al_1$-LDO	28.1	27	96
8	$Al(OH)_3$	10.2	8.5	83.3
9	$Mg(OH)_2$	4	3.5	87.5
10	$Cu(OH)_2$	3.5	3.2	91.8
11	Nano-Cu	6.8	6.5	95.5
12	Cu_2O	1.6	1.4	87.5

[a]Reaction conditions: catalyst (0.1 g), FAL (0.1 ml), 2-PrOH (20 mL), 160 °C, 6 h.

[b] Conversion, yield and selectivity were obtained by GC.

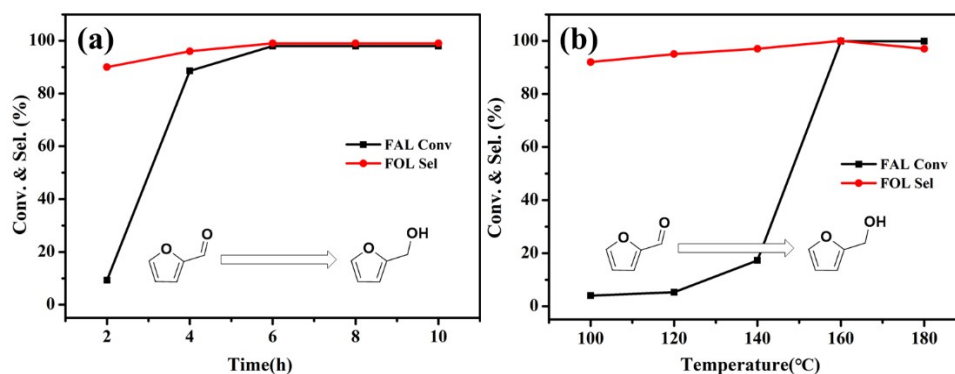[c]The catalyst was obtained after the LDH precursor was calcined at 500 °C.

Fig. S9 Effect of reaction time (a) and temperature (b) on the catalytic transfer hydrogenation of FAL to FOL. Reaction conditions: catalyst (0.1g), FAL (0.1mL), 2-PrOH (20 mL), 160 °C, 6 h.

As shown in Fig. S9a，when the reaction time was increased from 2 h to 10 h, the conversion rate of FAL increased from 10% to 99%, and the selectivity of FOL remained above 90%. When the reaction time reached 6 h, FAL was almost completely converted (>99%) with high FOL selectivity (>98%). At the same

9

time, the conversion of FAL increased with increasing temperature (Fig. S9b), which was attributed to the acceleration of the reaction rate by high temperature. The conversion of FAL increased slowly before 140 °C. When the reaction temperature reached 160 °C, the FAL was almost fully converted (>99%) with high furfural selectivity (>98%). But a higher temperature (180 °C) result in a significant decrease of FOL selectivity, because some hydroxyl aldehyde condensation products were produced at high temperature. Therefore, based on the above results, 160 °C and 6 h, respectively, were selected as the optimum reaction temperature and time. In addition, the effect of the amount of catalyst (0.02-0.12 g) was examined over the fresh $Cu_{1.5}Mg_{1.5}Al_1$-LDH catalyst at 160 °C with a reaction time of 6 h, and the obtained results were listed in Fig. S10†. The conversion of FAL first increases remarkably from 7.0 to 99% with the increase of catalyst loading (0.02-0.10 g). Meanwhile, the selectivity of FOL was basically maintained at 98%. However, when the amount of catalyst reached 0.12 g, the selectivity of FOL decreased slightly, which may be attributed to excessive catalyst can lead to the increase of the hydrogenation depth and affect the selectivity of FOL. Above all, under the optimal reaction conditions (20 mL of 2-PrOH, 0.1 g of the catalyst, 160 °C, and 6 h), the $Cu_{1.5}Mg_{1.5}Al_1$-LDH exhibited excellent FAL conversion (99%) and FOL selectivity (98%).
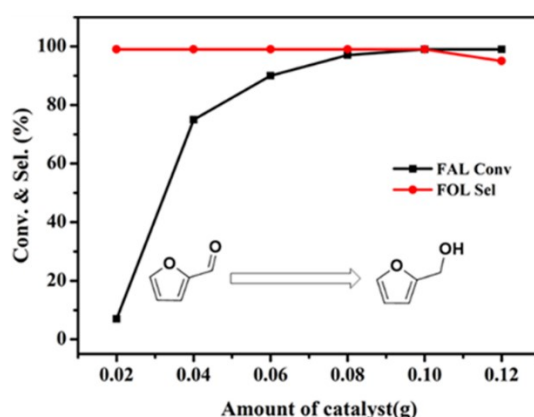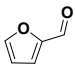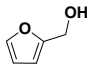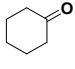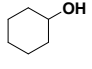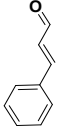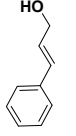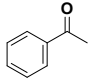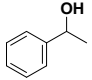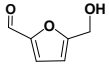

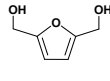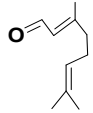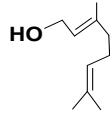**Fig. S10** Influence of the fresh $Cu_{1.5}Mg_{1.5}Al_1$-LDH catalyst dosage on FAL to FOL. Reaction conditions: FAL (0.1 mL), 2-PrOH (20 mL), 160 °C, 6 h.

Table S3. Selective hydrogenation of FAL to FOL in literature.

Catalyst	H Source	Temperature (°C)	Time (h)	Conversion (%)	Yield (%)	Selectivity (%)	Ref.
$Cu_{1.5}Mg_{1.5}Al_1$-LDH	2-PrOH	160	6	99	97.5	98.2	This Work
Cu/CuAl-MMO-400	2-PrOH	200	1	98	95.1	97.9	S1
Pd/Fe_2O_3	2-PrOH	180	7.5	68	41	60.3	S2
Al_2O_3-S(7)	2-PrOH	180	6	94.4	95.5	98.5	S3
$Al_7Zr_3@Fe_3O_4$(1/1)	2-PrOH	180	5	99.1	90.5	91.3	S4
NiO Nanoparticles	2-PrOH	170	1	100	94.6	94.6	S5
$PN\text{-}CeO_2$	2-PrOH	160	8	61	60.8	99.7	S6
Fe_3O_4-12	2-PrOH	160	5	97.5	90.1	92.4	S7
Ni–Fe (3/1) LDH	2-PrOH	140	5	77	61.1	91.9	S8
NiCoZn@CN-600	2-PrOH	130	8	100	>99	>99	S9

Table. S4. Catalytic transfer hydrogenation of Carbonyl compounds by the fresh $Cu_{1.5}Mg_{1.5}Al_1$-LDH.

Entry	Reactant	Main Product	Conversion (%)	Yield (%)
1			99.9	98.2
2			99.9	98.8
3			99.9	96.5
4			99.9	97.9
5			86.1	98.2
6			82.5	96.8

Reaction conditions: catalyst (0.1 g), substrate (0.1 ml), 2-PrOH (20 mL), 160 °C, 6 h.
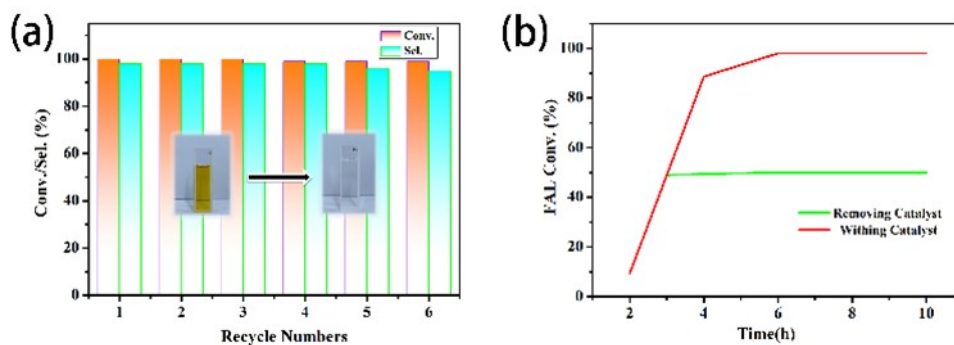
Fig. S11 Catalyst recycling (a) and a hot-filtration test (b) of $Cu_{1.5}Mg_{1.5}Al_1$-LDH in catalytic transfer hydrogenation of FAL under the optimized conditions.

In order to evaluate the stability of the catalyst, the $Cu_{1.5}Mg_{1.5}Al_1$-LDH cycle stability test was performed. At the end of the first catalytic reaction, the catalyst was separated by filtration and washed with absolute ethanol, then dried under vacuum at 80 °C for 6 h, and then used directly in the next experiment and in subsequent cycles. As depicted in Fig. S11a, the recycled $Cu_{1.5}Mg_{1.5}Al_1$-LDH catalyst could afford a 99% FAL conversion and 98% FOL selectivity after 6 cycles, indicating that the catalyst still maintains robust stability and excellent catalytic activity during recycle.

At the same time, the thermal filtration experiment was carried out (Fig. S11b). After 3 hours of reaction, the catalyst was filtered out and the subsequent reaction was observed. It was found that the conversion rate of FAL did not increase and remained unchanged, which also proved that the catalyst had good cycle stability
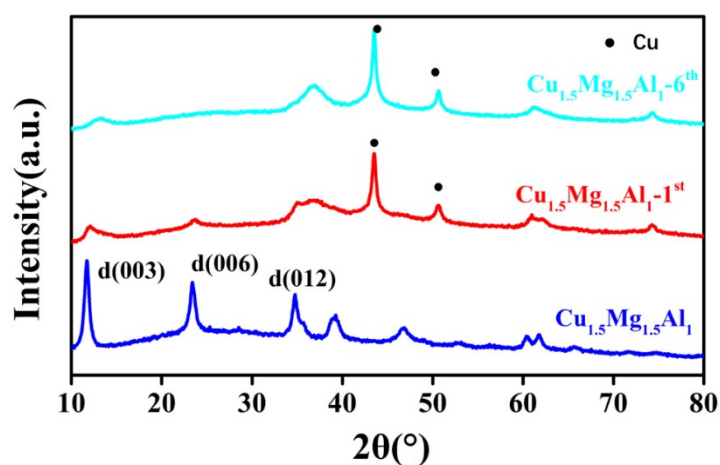

Fig. S12. XRD patterns of the fresh catalyst, the first cycle catalyst and the sixth catalyst.
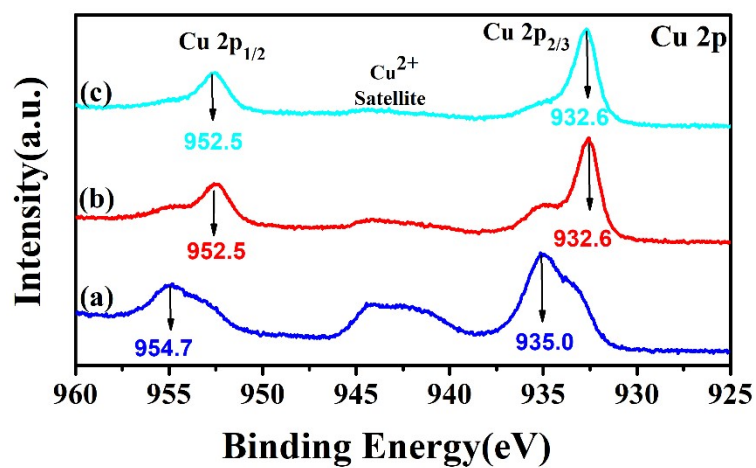
Fig. S13. XPS Cu 2p spectra of the fresh catalyst(a), the first cycle catalyst (b) and the sixth cycle catalyst(c).
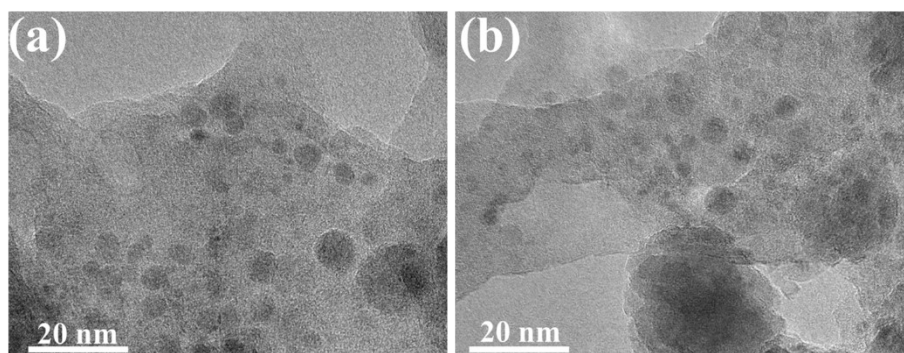

Fig. S14. TEM images of the first cycle catalyst and the sixth cycle catalyst.
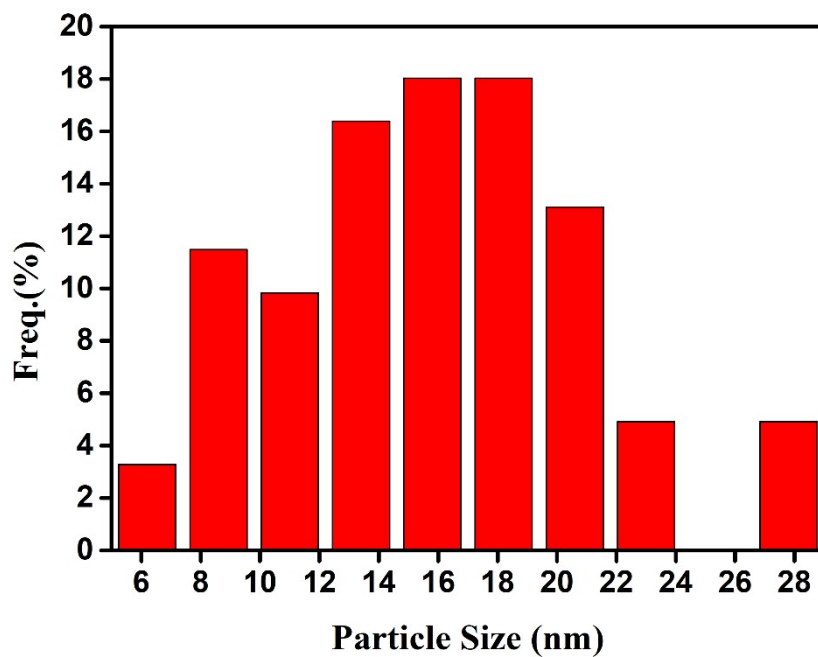
Fig. S15. The particle size distribution of in-situ reduced $Cu_{1.5}Mg_{1.5}Al_1$-LDH.

XRD analysis was performed on the sixth cycle catalyst confirmed the strength of the diffraction peak of metallic copper increased because more Cu^{2+} species are reduced to Cu^0 with increasing reaction times (Fig. S12). Moreover, the recycled catalyst was analyzed by XPS after the sixth cycle, and it has two peaks at 932.6 eV (Cu 2p3/2) and 952.5 eV (Cu 2p1/2), corresponding to Cu^+ and Cu^0 (Fig. S13). In addition, the Cu^{2+} satellite peaks almost disappeared, suggesting that the Cu^{2+} species in the fresh catalyst is reduced to the lower copper species. Finally, TEM images showed that the copper nanoparticles were slightly agglomerated and enlarged in the catalyst during the sixth cycle compared to the catalyst after the first in-situ reduction (Fig. S14). It is obvious that the average particle size of copper in the catalyst after the sixth cycle increased from 4.0 nm to 15.8 nm compared with the initial catalyst (Fig. S15). Although the particle size of copper increased, the catalytic performance was not affected.

References

1. Y. Y. Ren, Y. S. Yang, L. F. Chen, L. Wang, Y. W. Shi, P. Yin, W. L. Wang, M. F. Shao, X. Zhang and M. Wei, *Appl. Catal. B-Environ.*, 2022, 314, 11.

2. M. S. Kim, F. S. H. Simanjuntak, S. Lim, J. Jae, J. M. Ha and H. Lee, *J. Ind. Eng. Chem.*, 2017, 52, 59-65.

3. D. Scholz, C. Aellig and I. Hermans, *ChemSusChem*, 2014, 7, 268-275.

4. J. He, H. Li, A. Riisager and S. Yang, *ChemCatChem*, 2018, 10, 430-438.

5. J. He, L. Schill, S. Yang and A. Riisager, *ACS Sustain. Chem. Eng.*, 2018, 6, 17220-17229.

6. Y. Zou, M. K. Zhang, Y. X. Liu, Y. Y. Ma, S. Zhang and Y. Q. Qu, *J. Catal.*, 2022, 410, 54-62.

7. M. W. Ma, P. Hou, P. Zhang, J. J. Cao, H. Liu, H. J. Yue, G. Tian and S. H. Feng, *Appl. Catal. A-Gen.*, 2020, 602, 10.

8. T. Wang, A. Y. Hu, H. J. Wang and Y. M. Xia, *J. Chin. Chem. Soc.*, 2019, 66, 1610-1618.

9. S. J. Li, Y. F. Fan, C. H. Wu, C. F. Zhuang, Y. Wang, X. M. Li, J. Zhao and Z. F.

Zheng, *ACS Appl. Mater. Interfaces*, 2021, 13, 8507-8517.